Shahid Chamran University of Ahvaz

Iranian Association of Electrical and Electronics Engineers

Journal of Applied Research in Electrical Engineering

E-ISSN: 2783-2864
P-ISSN: 2717-414X
Homepage: https://jaree.scu.ac.ir/

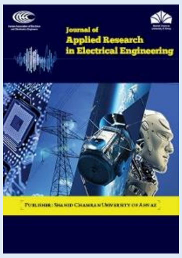

Research Article

Improvement of IBC-SHJ Solar Cell Efficiency Based on Back Contacts Geometry Engineering

Pegah Paknazar, Maryam Shakiba *, and Gholamreza Shaloo

Department of Electrical and Computer Engineering, Jundi-Shapur University of Technology, Dezful, Iran

** Corresponding Author: shakiba@jsu.ac.ir*

Abstract: In this study, the effect of the width of the n- and p-strips and gap between the electrodes on output characteristics of the IBC-SHJ solar cell including short-current current density, open-circuit voltage, fill factor and efficiency was investigated using Silvaco ATHENA and ATLAS simulation software. In this regard, the efficiency of the IBC-SHJ solar cell was improved by developing the geometry of the back contacts. The values for the short-circuit current density, open-circuit voltage, fill factor and efficiency of the solar cell were analysed using physical phenomena and the distribution of the electric field and electric potential for the aforementioned parameters. The results have shown that the width of the n- and p-strips is one of the most effective parameters for improving the efficiency improvement. Moreover, a maximum efficiency of 23.52% was achieved for IBC-SHJ with improved solar cell parameters, focusing on the elimination of additional ARCs and greater structural periodicity. Thus, a simple structure with no complexity in the fabrication process is proposed. The results show that the best width of the p-strip, n-strip and gap between the electrodes is 400 µm, 80 µm and 30 µm, respectively, to achieve improved efficiency.

Keywords: Back contacts geometry engineering, p-strip width, n-strip width, gap width, IBC-SHJ solar cell, cell efficiency

Article history
Received 14 April 2024; Revised 22 August 2024; Accepted 06 September 2024; Published online 23 October 2024.

How to cite this article
P. Paknazar, M. Shakiba, and G. Shaloo, " Improvement of IBC-SHJ Solar Cell Efficiency Based on Back Contacts Geometry Engineering," *J. Appl. Res. Electr. Eng*., Vol. 3, No. 1, pp. 83-89, 2024. DOI: 10.22055/jaree.2024.46609.1115

1. Introduction

The main renewable energy sources such as wind and solar energy are not only abundant and affordable, but are also considered a suitable alternative to fossil fuels. Among the renewable energy sources, solar energy has a high potential to be converted into other types of energy [1-3]. So far, much research has been done to increase the efficiency of silicon solar cells with the common finger contact structure [4-5]. In recent years, the design of the contact geometry of the cell has been one of the areas of interest for researchers to achieve optimal efficiency [6-7]. One of the most important structures presented in this field is the silicon heterojunction solar cell with interdigitated back contacts [7]. The fact that all contacts are arranged behind the cell eliminates the shadow effect and increases the short-circuit current [8]. In addition, the use of the heterojunction structure leads to an increase in the open circuit voltage due to the use of the intrinsic hydrogenated a-Si buffer layer [8]. Over the past 10 years, research has been conducted to increase the efficiency of IBC-SHJ cells. In 2013, Silvaco presented the IBC-SHJ cell with an efficiency of 20.43% [8]. In 2016, M. Belarbi et. al. achieved an efficiency of 23.20% by improving the cell deposition parameters [9]. Taking into account a periodicity of the IBC-SHJ structure and simultaneously adding further layers and anti-reflective coatings with textured structures on the front side as well as the use of TCO layers in the rear part of the cell, an efficiency of 27.41% was achieved by J. Bao et. al. in 2020 [10]. The removal of the amorphous silicon layers and the use of a silver contact in addition to the aluminium contact for increase the cell current, modelling two samples of IBC solar cells including planar and pyramidal textured ones, with a focus on optimizing the texturing of the front surface. In [11], A. R. M. Rais et. al. reported that the efficiency of planar and pyramidal textured solar cells were 22.36% and 23.31%, respectively [11]. However, it should be noted that the increase in efficiency in the studies [10] and [11] requires an increase in the complexity of the structure, the manufacturing cost due to the use of silver contacts and thus an increase in the challenges of the manufacturing process. In this research work, the aim is to design and simulate an improved silicon heterojunction solar cell with interdigitated back contacts, which has the simplest structure compared to other research works and also has the least fabrication challenges. In fact, the efficiency of the IBC-SHJ solar cells have been improved by developing the geometry of the back contacts. In this regard, the effect of the width of the n- and p-strip and gap between the electrodes on the output characteristics of the IBC-SHJ solar cell including J_{sc}, V_{oc}, *FF* and *Eff* have been investigated. To model the IBC-SHJ solar cell, ATHENA and ATLAS toolboxes have been used, respectively, to deposit different layers of the cell and simulate its electrical behavior in Silvaco software. To increase the accuracy of the simulation of the structure, the trap levels of the amorphous silicon layers have been modelled. MATLAB software was also used to draw the diagrams as accurately as possible. In the second part of this research, the analysis of the electric field distribution and its effect on the charge carrier transport in the IBC-SHJ cell is presented. In the third part, the mathematical relationships that determine the density of states (DOS) model and the particle transport have been investigated. In the fourth part, the effect of the width of the n- and p-strip and gap between the electrodes on the output characteristics of the IBC-SHJ solar cell including J_{sc}, V_{oc}, *FF* and *Eff* have been investigated. In addition, the results were compared with those of previous studies. In the fifth section, the main results of the proposed IBC-SHJ cell structure are presented.

2. Analysis of Electric Field Distribution and Its Effect on Carrier Transport

To create anode and cathode electrodes, a structure of n-type and p-type layers of hydrogenated a-Si is deposited on the back side of the IBC-SHJ cell so that the layers are one in between. Depending on the doping concentration of the c-Si substrate, these n- and p-type layers play the role of the emitter or the back surface field (BSF). As shown in Figure 1, the width of the elementary structure (pitch) of the cell is equal to the distance between the opposing electrodes, taking into account the gap between them. It is possible to create the periodicity in more complex structures, which of course poses more challenges in fabrication. In this research, the dimensions and the type of materials used in the different layers have been selected according to the criterion of reproducibility, so that the simulation results can contribute to the improvement of the fabrication process [12].

It is worth noting that in Fig. 1, the thickness of SiN_x, n-type c-Si, defective c-Si, i-a-Si, emitter/a-Si, BSF/a-Si, and electrode/Al layers are 75 nm, 150 µm, 1 nm, 6 nm, 20 nm, 20 nm, 0.2 µm, respectively. Moreover, the optimal doping concentration of the emitter and BSF regions is 2×10^{19} cm^{-3} and 4.3×10^{18} cm^{-3}, respectively. The substrate used to improve deposition parameters is an n-type c-Si wafer with a thickness of 300 μm and a width of 1750 μm, which is equivalent to one cell pitch. The resistivity of the substrate is equal to 2 $\Omega.cm$.

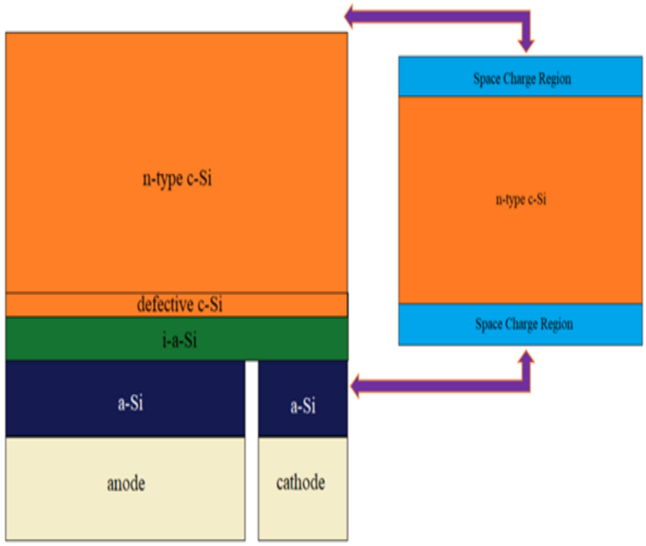

Fig. 1. Schematic of the simulated IBC-SHJ structure along with the approximated regions of space charge in the upper and lower areas of the cell

Also, using n-type c-Si substrate will lead to an increase in V_{oc} as a result of increasing efficiency [13] [14]. On the front surface of the cell, a SiN_x layer with a thickness of 75 *nm* has been used as an anti-reflection coating, for this purpose, the physical model of concentration mobility (CONMOB) has been used in the simulation [15-17]. Therefore, due to not choosing the same type of impurity for ARC layers and c-Si substrate, the existence of an electric field on the top of the cell that leads to more drift of the photocarriers and prevents their recombination will be inevitable. According to Figure 1, the presence of anti-reflection coating with the opposite doping concentration of the substrate leads to the creation of a space charge region in the front part of the cell. The internal electric field created in this space charge region will prevent the recombination of the generated photocarriers and move them towards the back contacts of the cell. Also, near the back contacts, due to the presence of the back p-n junction, another space charge region is created, which facilitates the drift of the electron and hole carriers towards the electrode of the same name, and by preventing the recombination of photocarriers, it will increase the photocurrent of the cell.

As shown in Figure 2(a) and 2(b), the distribution of electric field and potential at the rear of back contact prevent the recombination of photocarriers. In fact, the design of two space charge areas in the upper and lower parts of the cell, in addition to preventing the recombination of photocarriers, leads to drift them towards the interdigitated back contacts.

Consideration of electric field distribution of IBC-SHJ solar cell structure is so important. In the front part of the cell where there is the maximum photo generation rate, the electric field increases so that the photocarriers are separated and reach the back contacts with the lowest recombination rate. Also, the electric field reaches its maximum value near the back contacts; because in this part of the structure, the amount of carrier collection in metal contacts must reach its highest value. Therefore, the electric field must be large enough to collect more photocarriers at the metal contacts by separating them as much as possible.

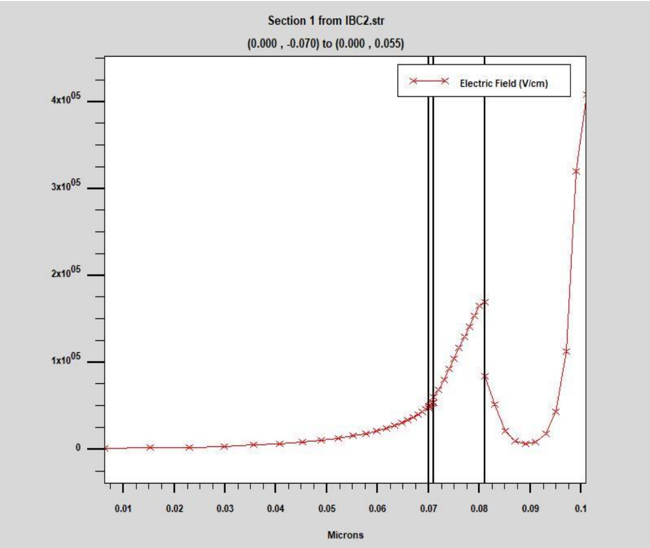

Fig. 2(a). Electric field distribution of space charge region at the rear of back contacts

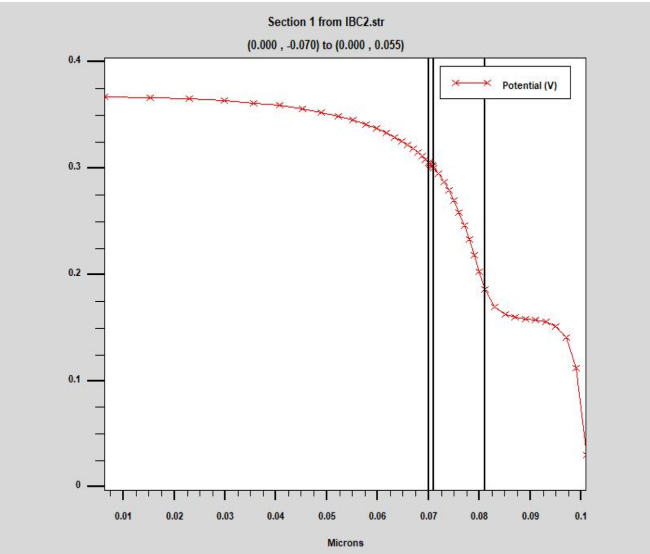

Fig. 2(b). Electric potential distribution of space charge region at the rear of back contacts

3. PHYSICAL MODELS AND EQUATIONS USED IN SIMULATION

3.1. Physical Models

In order to match the numerical modelling and experimental results as much as possible, in this research, we have tried to use accurate physical models to describe the behaviour of IBC-SHJ cells. In this regard, the band gap narrowing (BGN) model has been used to reduce the energy gap [8]. In fact, the narrowing of the band gap shows how applying a high doping concentration (greater than 10^{18} cm^{-3}) changes the band gap by reducing the energy of the conduction band and increasing the energy of the valence band [8]. On the other hand, in order to model different recombination mechanisms, Fermi, Shockley-Read-Hall (SRH), Auger and surface recombination models are also included in the simulation. Meanwhile, carrier recombination is also modelled as a function of doping concentration via SRH and Auger mechanisms [18-20].

Disordered materials such as amorphous silicon contain a large amount of defect states in their energy band gap. Therefore, the density of state (DOS) model in the energy bandgap is used to model amorphous silicon devices. The density model of the defect states is described as a combination of the tail of the band using the exponential decay function and the mid of the band using the Gaussian distribution function. It is assumed that the total density of states, $g(E)$, is composed of four bands: two tail bands (a donor-like valence band and an acceptor-like conduction band) and two deep level bands (one acceptor-like and the other donor-like) which are modelled using a Gaussian distribution. *g(E)* is modeled according to relation (1) [8]:

$$g(E) = g_{TA}(E) + g_{TD}(E) + g_{GA}(E) + g_{GD}(E) \qquad (1)$$

In relation (1), E is the trap energy, E_C is the conduction band energy, E_V is the valence band energy and the subscripts (T, G, A, D) stand for tail, Gaussian (deep level), acceptor and donor states respectively. The components of $g(E)$ are defined as follows [15]:

$$g_{TA}(E) = N_{TA} exp\left[\frac{E - E_C}{W_{TA}}\right] \qquad (2)$$

$$g_{TD}(E) = N_{TD} exp\left[\frac{E_V - E}{W_{TD}}\right] \qquad (3)$$

$$g_{GA}(E) = N_{GA} exp\left[-\left[\frac{E_{GA} - E}{W_{GA}}\right]^2\right] \qquad (4)$$

$$g_{GD}(E) = N_{GD} exp\left[-\left[\frac{E - E_{GD}}{W_{GD}}\right]^2\right] \qquad (5)$$

For an exponential tail distribution, the DOS is described by its conduction and valence band edge intercept densities (N_{TA} and N_{TD}), and by its characteristic decay energy (W_{TA} and W_{TD}). For Gaussian distributions, the DOS is described by its total density of states (N_{GA} and N_{GD}), its characteristic decay energy (W_{GA} and W_{GD}), and its peak energy distribution (E_{GA} and E_{GD}). The energy distribution of exponential band tail and Gaussian distribution of trap states in the middle of the energy gap are key parameters for high accuracy simulation.

For the c-Si/a-Si interface on the back surface, the thermionic emission model has been used, in which the distribution function of the defect states at the interface of two layers, one for holes and the other for electrons, is modeled. In order to model the interface between the defects-free crystalline silicon layer and the amorphous silicon layer as much as possible, a defective c-Si thin layer has been used between the two layers [15]. The Sopra database is also used for the refractive index of a-Si layers [21, 22]. AM1.5G solar spectrum has been used to simulate sunlight in standard conditions with a light intensity of 1000 W/m^2 and a temperature of 26˚*C*.

3.2. Equations of Carrier Transport

The specialized software used in this research to design and simulation the IBC-SHJ solar cell is Silvaco software. The Athena tool in this software models and simulates the fabrication process in the Monte Carlo method and in conditions very similar to the new technologies presented in the field of semiconductor devices fabrication. In addition, the Atlas tool simulates the electrical behaviour of cell designed in Athena. It uses the drift-diffusion model based on the discretization of differential equations and solving equations using numerical solutions such as Gumel, Newton-Raphson and Block methods. Output characteristics extracted from Atlas tool are Fill Factor (*FF*) and Efficiency (η) obtained from relations (6) and (7) respectively [15,19]:

$$FF = \frac{V_{mpp}I_{mpp}}{V_{oc}I_{sc}} \quad (6)$$

$$\eta = \frac{P_{out}}{P_{in}} = \frac{V_{oc}I_{sc}FF}{P_{light}} \quad (7)$$

In relation (6), V_{mpp} and I_{mpp} represent the voltage and current at the maximum power point, respectively.

Three sets of basic equations are used to simulate the solar cell in the Silvaco software based on the drift-diffusion model. These equations are: Poisson's equation, carrier's continuity equations and transport (current) equations. Poisson's equation specifies the relationship between electrostatic potential (ψ) and the space charge density (ρ) and is expressed as follows [19]:

$$div(\varepsilon \nabla \psi) = -\rho \quad (8)$$

In relation (8), ε is the permeability coefficient of the environment. The local space charge density represents carriers (electrons and holes) and ionized impurities. On the other hand, carriers continuity equations specify the gradient of electron and hole carriers in terms of time and are defined as follows [8]:

$$\frac{\partial n}{\partial t} = \frac{1}{q} div\vec{J_n} + G_n - R_n \quad (9)$$

$$\frac{\partial p}{\partial t} = -\frac{1}{q} div\vec{J_p} + G_p - R_p \quad (10)$$

In relations (9) and (10), n and p are electrons and holes concentration respectively. J Indicates the current density, G indicates the photo generation rate and R indicates the recombination rate for the respective carriers. Electric charge is also represented by q. Also, the transport equations that determine the gradient of electron and hole carriers in terms of location and are defined as follows [15]:

$$\vec{J_n} = q\mu_n nE + qD_n \nabla n(x) \quad (11)$$

$$\vec{J_p} = q\mu_p pE - qD_p \nabla p(x) \quad (12)$$

In relations (11) and (12), μ_n and μ_p are electron and hole mobilities, respectively, E is electric field and D_n and D_p are electrons and holes diffusion coefficients, respectively.

3.3. Ray Tracing

Ray tracing is one of the simplest models of optical simulation. In this study, the ray tracing optical model has also been employed. This optical model primarily disregards the wave nature of light and traces direct paths towards rays passing through boundaries. Reflected and transmitted components are calculated based on the Fresnel equations, and incoming rays at each boundary are divided into two parts. Following these steps, the system traces the trajectories of both these rays. The simplified Fresnel equations with Snell's laws are as follows:

$$r_p = -\frac{tan(\theta_i - \theta_t)}{tan(\theta_i + \theta_t)} \quad (13)$$

$$t_p = \frac{2\,sin\,\theta_t\,cos\,\theta_i}{sin(\theta_i + \theta_t)\,cos(\theta_i - \theta_t)} \quad (14)$$

$$r_s = -\frac{sin(\theta_i - \theta_t)}{sin(\theta_i + \theta_t)} \quad (15)$$

$$t_s = \frac{2\,sin\,\theta_t\,cos\,\theta_i}{sin(\theta_i + \theta_t)} \quad (16)$$

In the equations for r_p and r_s, representing the reflection of p- and s-polarized rays, t_p and t_s indicate the transmission of p- and s-polarized rays, respectively. θ_i and θ_t denote the angles of incidence and transmission with respect to the surface normal vector. Also, reflecting and refracting rays each present at their respective angles relative to the surface normal vector. The incident angles are also specified in the equations in this illustration. The refractive index of the upper medium (n_1, smaller than the refractive index of the lower medium n_2), is such that the refracted ray approaches the normal vector of the boundary.

4. Results and Discussion

In this research, in order to improve the characteristics of the IBC-SHJ cell, one of the most effective parameter as the width of the n- and p-strip and the gap width between electrodes are improved.

In the following, the influence of the mentioned parameters on the output characteristics of J_{sc}, V_{oc}, *FF* and *Eff* is investigated to improve the efficiency of the IBC-SHJ solar cell. It should be noted that to investigate the effect of each parameter, other parameters of the cell are considered constant.

4.1. Effect of p-Strip Width

The J_{sc}, V_{oc}, *FF* and *Eff* graphs considered with the change of p-strip width are presented in Figure 3.

Increasing the width of p-strip, increases the current. But at the same time, it does not have much effect on the voltage. As can be seen in Figure 3, J_{sc} increases with increasing the p-strip width. Because the width of metal contact is equal to the p-strip. On the other hand increasing the width of metal contact decreases the cell series resistance and thus, increases the cell current. Generally, in the IBC-SHJ structure, the p-strip width is set to be larger than the n-strip width. Holes are the minority carriers of the substrate. By choosing a larger width for the p-strip region, it will be possible to collect more minority carriers in the metal contacts. It significantly reduces the possibility of recombination in the substrate and this leads to an increase the cell current. Meanwhile, V_{oc} increases with increasing the p-strip width. But the voltage increase is very small and insignificant. Increasing the width of p-strip does not have much effect on the voltage. On the other hand, the *FF* decreases as the p-strip width increases. Because, increasing the width of p-strip, increases I_{sc}. Therefore, according to relation (6), *FF* decreases. Also, the efficiency of the cell decreases with the increase of the p-strip width. Considering the simulation, the most optimal value for p-strip width is equal to 400 μm.

4.2. Effect of Gap Width between Electrodes

The width of the gap between the electrodes is one of the key parameters in controlling the current of the cell. Because

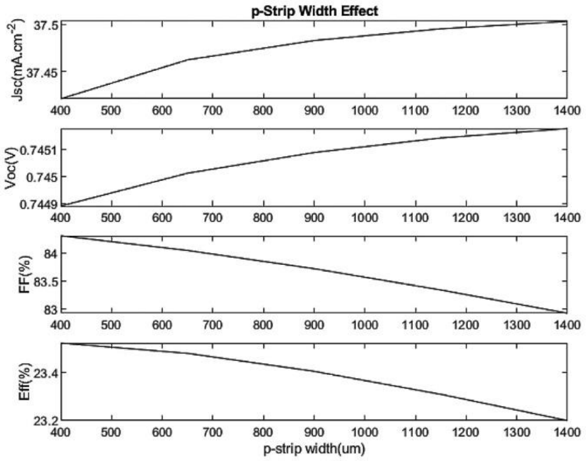

Fig. 3. Effect of p-strip width on *Jsc*, *Voc*, *FF* and *Eff*, the doping concentration of Emitter and BSF regions is equal to 2×10^{19} cm^{-3} and 4.3×10^{18} cm^{-3} respectively.

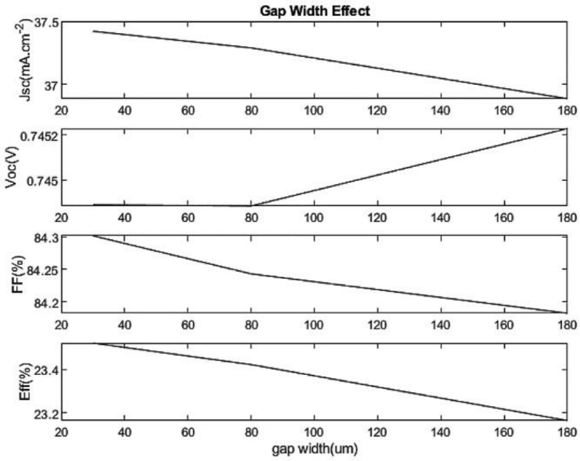

Fig. 4. Effect of gap width on J_{sc}, V_{oc}, *FF* and *Eff*, doping concentration of Emitter and BSF regions is equal to 2×10^{19} cm^{-3} and 4.3×10^{18} cm^{-3} respectively.

it can lead to shunting the electrodes if it not adjusted accurately. On the other hand, its excessive increase reduces the photocurrent by reducing the optimal value of the n- and p-strip width and increasing the cell series resistance. Next, the J_{sc}, V_{oc}, *FF* and *Eff* graphs considering the change of gap width between the electrodes are presented in Figure 4. Increasing the gap width between the electrodes leads to decrease the current but does not have a great effect on the voltage. As shown in Figure 4, J_{sc} decreases with increasing gap width. In fact, the gap region between the electrodes has an important effect on the photocurrent of the cell by influencing the n- and p-strip width. On the other hand, due to the increase in cell resistance, V_{oc} increases with a low slope.

According to Figure 4, as the gap width increases, I_{sc} increases and thus, *FF* decreases. Also, cell efficiency decreases. Because the recombination of the minority carriers between the p- and the n-strip increases due to the increase in the lateral distance travelled. In other words, the increase of the gap width corresponds to an additional lateral distance for the minority photocarriers generated in the c-Si substrate and in the upper part of the n-strip. This extra distance increases the probability of recombination before reaching the p-strip. In addition, by increasing the width of the gap between the electrodes, the possibility of recombination at the interface between the c-Si substrate and the gap region increases. Therefore, according to all reasons mentioned above, the gap width should be set as low as possible to obtain the optimal value for cell efficiency. As a result, the most optimal value for the gap width equal to 30 μm is obtained.

4.3. Effect of n-Strip Width

The J_{sc}, V_{oc}, *FF* and *Eff* graphs with changing the n-strip width are presented in Figure 5. Increasing the n-strip width increases the cell current. But it has little effect on the voltage. In this situation, due to the increase of the average lateral distance that the minority carriers must travel to reach the p-strip, J_{sc} decreases and increases the probability of carrier recombination and decreases the cell current. According to the V_{oc} graph, V_{oc} decreases with a small slope. As the n-strip width increases to 580 μm, *FF* increases and then decreases. Because its increase up to 580 μm, increases the I_{mpp} and for more than 580 μm, I_{sc} increases. Therefore, according to relation (6), it can be seen that *FF* increases until reaching a width of 580 μm and then decreases from this value. On the other hand, the efficiency decreases with the decrease of J_{sc}. Therefore, the n-strip should be set as low as possible to obtain the best J_{sc} values. In fact, a larger width leads to an increase in series resistance against with the current of majority carriers (electrons). As a result, the most optimal value for the n-strip width is equal to 80 μm. Therefore, in the proposed IBC-SHJ solar cell, the most improved value for the width of p-strip, gap and n-strip is equal to 400μm, 30μm and 80μm respectively. Proposed values of IBC-SHJ cell efficiency at Different p-strip, gap and n-strip widths are given in Tables 1, 2 and 3 respectively. Also in Table 4, the width of p-strip, gap and n-strip and Efficiency of the proposed IBC-SHJ solar cell compared to previous research.

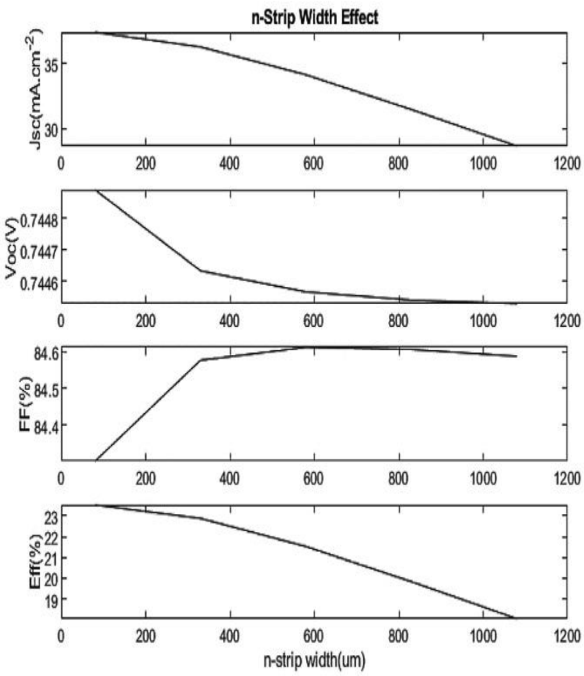

Fig. 5. Effect of n-strip width on J_{sc}, V_{oc}, *FF* and *Eff*, doping concentration of Emitter and BSF regions is equal to 2×10^{19} cm^{-3} and 4.3×10^{18} cm^{-3} respectively.

Table 1: IBC-SHJ Cell Efficiency at Different p-Strip Width

p-Strip width (µm)	Efficiency (%)
400	23.52
650	23.48
900	23.40
1150	23.31
1400	23.20

Table 2 : IBC-SHJ Cell Efficiency at Different Gap Width

Gap width (µm)	Efficiency (%)
30	23.52
80	23.42
180	23.16

Table 3 : IBC-SHJ Cell Efficiency at Different n-Strip Width

n-Strip width (µm)	Efficiency (%)
80	23.52
330	22.88
580	21.53
830	19.83
1080	18.05

As mentioned preview and as shown in Table 4, in the proposed IBC-SHJ solar cell, the most improved value for the width of p-strip, gap and n-strip is equal to 400μm, 30μm and 80μm respectively. Generally, in the IBC-SHJ structure, the p-strip width is set to be larger than the n-strip width. Because holes are the minority carriers of the substrate then by choosing a larger width for the p-strip region, it will be possible to collect more minority carriers in the metal contacts. It significantly reduces the possibility of recombination in the substrate and this leads to an increase the cell current and cell efficiency. On the other hand, the gap region between the electrodes has an important effect on the photocurrent of the cell by influencing the n- and p-strip width. Because the recombination of the minority carriers between the p- and the n-strip increases due to the increase in the lateral distance travelled. In other words, the increase of the gap width corresponds to an additional lateral distance for the minority photocarriers generated in the c-Si substrate and in the upper part of the n-strip. Finally, increasing the n-strip width, due to the increase of the average lateral distance that the minority carriers must travel to reach the p-strip, J_{sc} decreases and increases the probability of carrier recombination and decreases the cell current.

Table 4 : The Width of p-Strip, Gap and n-Strip and Efficiency of the Proposed IBC-SHJ Solar Cell Compared with Previous Stuctures

Ref.	Parameters			
	p-Strip width(µm)	Gap width (µm)	n-Strip width (µm)	Efficiency (%)
[8]	1200	50	500	20.43
[9]	950	50	180	23.20
[Proposed structure]	400	30	80	23.52

Therefore, the n-strip should be set as low as possible to obtain the best J_{sc} values.

5. Conclusion

In this research, one of the most effective parameters for the efficiency of the IBC-SHJ cell was investigated, namely the width of the n- and p-strip and the gap width between the electrodes. Our improved IBC-SHJ solar cell yields a short-circuit current density of 37.42 mA/cm^2 and an open-circuit voltage of 745 mV with a cell efficiency of 23.52% and a fill factor of 84.30 under AM1.5G without additional ARCs and more structural periodicity. Thus, a simple structure with improved conversion efficiency is proposed. The simulation shows that the efficiency of the cell depends on the width of the p-strip, gap and n-strip, so these parameters can be improved accordingly. The results show that the optimum width of the p-strip, the gap between the electrodes and the n-strip is 400µm, 30µm and 80µm respectively. The presence of an antireflective coating with the opposite concentration of the substrate, by creating a space charge region and its electric field in the front part of the cell, prevents the photocarriers from recombining and drifts them to the rear contacts of the cell, so that they are collected in the rear contact of the same name due to the existence of the rear p-n junction and the resulting electric field.

Credit Authorship Contribution Statement

Pegah Paknazar: Data curation, Formal analysis, Investigation, Project administration, Resources, Software, Validation, Visualization, Roles/Writing - original draft. **Maryam Shakiba**: Conceptualization, Investigation, Methodology, Supervision, Writing - review & editing. **Gholamreza Shaloo**: Data curation, Formal analysis, Software, Validation, Visualization.

Declaration Of Competing Interest

The authors declare that they have no known competing financial interests or personal relationships that could have appeared to influence the work reported in this paper. The ethical issues; including plagiarism, informed consent, misconduct, data fabrication and/or falsification, double publication and/or submission, redundancy has been completely observed by the authors.

References

[1] T. Allen, J. Bullock, X. Yang, A. Javey, S. De Wolf, “Passivating contacts for crystalline silicon solar cells”, Nature Energy, vol. 4, pp. 914-928, 2019.

[2] C. N Kruse, S. Schafer, F. Haase, V. Mertens, H. Schulte-Huxel, B. Lim, B. Min, T. Dullweber, R. Peibst, R. Brendel, “ Simulation-based roadmap for the intergration of poly-silicon on oxide contacts into screen-printed crystalline silicon solar cells”, Nature research, vol. 11, pp. 996, 2021.

[3] Maryam. Shakiba, Mohsen. Shakiba, “Role of Critical Processing Parameters on Fundamental Phenomena and Characterizations of DC Argon Glow Discharge”, Optoelectronical Nanostructures, vol. 7, pp. 67-91, 2022.

[4] Younes Menni, Ahmed AZZI, Ali J.Chamkha, “A Review of Solar Energy Collectors: Models and Applications”, Journal of Applied and Computational Mechanics, October 2018 Pages 375-401.

[5] V. Giglia, R. Varache, J. Veirman, E. Fourmond, “Influence of cell edges on the performance of silicon heterojunction solar cells”, Solar Energy Materials and Solar Cells, vol. 238, pp. 111605, 2022.

[6] M. Shakiba, A. Kosarian, E. Farshidi, "Effects of processing parameters on crystalline structure and optoelectronic behavior of DC sputtered ITO thin film", J Mater Sci: Mater Electron, vol. 28, pp. 787-797, 2016.

[7] Ana. Pavlovic, Cristiano. Fragassa, Marco. Bertoldi, Vladyslav Mikhnych, "Thermal Behavior of Monocrystalline Silicon Solar Cells: A Numerical and Experimental Investigation on the Module Encapsulation Materials", Journal of Applied and Computational Mechanics, July 2021, Pages 1847-1855.

[8] silvaco.com. (July 01, 2013). https://silvaco.com/dynamicweb/jsp/downloads/DownloadDocStepsAction.do?req=download&nm=simstd_Q3_2013_a2.pdf

[9] M. Belarbi, M. Beghdad, A. Mekemeche, "Simulation and optimization of n-type interdigitated back contact silicon heterojunction (IBC-SiHJ) solar cell structure using Silvaco Tcad Atlas", Solar Energy, vol. 127, pp. 206-215, 2016.

[10] J. Bao, A. Liu, Y. Lin, Y. Zhou, "An insight into effect of front surface field on the performance of interdigitated back contact silicon heterojunction solar cells", Materials Chemistry and Physics, vol. 255, pp. 123625, 2020.

[11] A. R. M Rais, S. Sepeai, M. K. M Desa, M. A Ibrahim, P.J Ker, S. H Zaidi, K. Sopian, "Photo-generation profiles in deeply-etched, two-dimensional patterns in interdigitated back contact solar cells", Journal of Ovonic Research, vol. 17, pp. 283-289, 2021.

[12] C. Hollemann, F. Hasse, M. Rienacker, V. Barnscheidt, J. Krugener, N. Folchert, R. Brendel, S. Ritcher, S. Grober, E. Sauter, J. Hubner, M. Oestreich, R. Peibst, "Separating the two polarities of the POLO contacts of an 26.1%-efficient IBC solar cell", Nature research, vol. 10, pp. 658, 2020.

[13] P. Procel, G. Yang, O. Isabella, M. Zeman, "Theoretical evaluation of contact stack for high efficiency IBC-SHJ solar cells", Solar Energy Materials and Solar Cells, vol. 186, pp. 66-77, 2018.

[14] A. Kosarian, M. Shakiba, E. Farshidi. "Role of hydrogen treatment on microstructural and opto-electrical properties of amorphous ITO thin films deposited by reactive gas-timing DC magnetron sputtering". J Mater Sci: Mater Electron. 28(2017) 10525–10534.

[15] M. Aurientis. Interdigitated back contact n-type solar cell with black silicon anti-reflecting layer: simulations and experiments. A Thesis submitted in partial fulfilment of the requirements for the degree of Master of Science in Technology. (2014).

[16] A. Kosarian, M. Shakiba, E. Farshidi. "Role of sputtering power on the microstructural and electro-optical properties of ITO thin films deposited using DC sputtering technique". IEEJ Transaction on Electrical and Electronic Engineering. 13(2018) 27–31.

[17] Mohsen. Makvandi, Mohammad. Javad Maleki, Mohammad. Soroosh, "Compact All-Optical Encoder Based on Silicon Photonic Crystal Structure", Journal of Applied Research in Electrical Engineering, January 2022, Pages 1-7.

[18] Zahra. Ahangari, "Performance Analysis of a Steep-Slope Bi-channel GaSb-GaAs Extended Source Tunnel Field Effect Transistor with Enhanced Band-to-Band Tunneling Current", Journal of Applied Research in Electrical Engineering, July 2023, Pages 206-213.

[19] M. Lu, U. Das, S. Bowden, S. Hegedus, R. Birkmire, "and colleagues of interdigitated back contact silicon heterojunction solar cells by two-dimensional numerical simulation", Institute of Energy Conversion, Univesity of Delaware, Newark, DE 19716 U.S.A, IEEE. 2009.

[20] T. Sawada, N. Terada, S. Tsuge, T. Baba, T. Takahama, K. Wakisaka, S. Tsuda, S. Nakano, "High-efficiency a-Si/c-Si heterojunction solar cell", In: Proceedings of 1994 IEEE 1st World Conference on Photovoltaic Energy Conversion, Waikoloa, USA, pp. 1219–1226, 1994.

[21] K. Yoshikawa, H. Kawasaki, W. Yoshida, T. Irie, K. Konishi, K. Nakano, T. Uto, D. Adachi, M. Kanematsu, H. Uzu, K. Yamamoto, "Silicon heterojunction solar cell with interdigitated back contacts for a photoconversion efiiciency", Nature Energy, vol. 2, pp. 17032, 2017.

[22] D. Diouf, J. P Kleider, C. Longeaud, "Two-dimensional simulations of interdigitated ack contact silicon heterojunctions solar cells", Chapter 15 of the book physics and technology of amorphous-crystalline silicon heterostructure solar cells, Springer. pp. 483-519, 2011.

BIOGRAPHY

Pegah Paknazar was born in Dezful, Khuzestan, Iran. She received the master degree in Electrical and electronic engineering with a focus on the field of semiconductor devices from the Jundi-Shapur University of Technology, Dezful, Iran in 2022. Her studies in the master thesis were done on the subject of increasing the efficiency of silicon heterojunction solar cell by designing and adjusting interdigitated back contacts and some of the results obtained in the studies were presented in this paper.

Maryam Shakiba was born in Dezful, Khuzestan, Iran. She received the Ph.D. degree in electronic engineering from the Shahid Chamran University of Ahvaz, in 2015. She is presently an Assistant Professor in electronic engineering in Jundi-Shapur University of Technology, Dezful, Iran. Her research interests include semiconductor electronics, especially amorphous silicon solar cells, intelligent system and analog integrated circuit.

Gholamreza Shaloo was born in Abadan, Iran. He completed his undergraduate education at Isfahan University in Iran in 2020 and his postgraduate education at Jundi-Shapur University of Technology, Dezful, Iran in 2024. His field of study at the graduate level was using intelligent system for modelling semiconductor device. The title of his thesis was modelling of IBC silicon solar cell based on artificial neural network.